HHS Public Access

Author manuscript

Aerosol Sci Technol. Author manuscript; available in PMC 2015 October 28.

Published in final edited form as:

Aerosol Sci Technol. 2012 April ; 46(4): 473–484. doi:10.1080/02786826.2011.639316.

Investigation of Aerosol Surface Area Estimation from Number and Mass Concentration Measurements: Particle Density Effect

Bon Ki Ku and **Douglas E. Evans**

Centers for Disease Control and Prevention (CDC), National Institute for Occupational Safety and Health (NIOSH), Cincinnati, Ohio, USA

Abstract

For nanoparticles with nonspherical morphologies, e.g., open agglomerates or fibrous particles, it is expected that the actual density of agglomerates may be significantly different from the bulk material density. It is further expected that using the material density may upset the relationship between surface area and mass when a method for estimating aerosol surface area from number and mass concentrations (referred to as “Maynard’s estimation method”) is used. Therefore, it is necessary to quantitatively investigate how much the Maynard’s estimation method depends on particle morphology and density. In this study, aerosol surface area estimated from number and mass concentration measurements was evaluated and compared with values from two reference methods: a method proposed by Lall and Friedlander for agglomerates and a mobility based method for compact nonspherical particles using well-defined polydisperse aerosols with known particle densities. Polydisperse silver aerosol particles were generated by an aerosol generation facility. Generated aerosols had a range of morphologies, count median diameters (CMD) between 25 and 50 nm, and geometric standard deviations (GSD) between 1.5 and 1.8. The surface area estimates from number and mass concentration measurements correlated well with the two reference values when gravimetric mass was used. The aerosol surface area estimates from the Maynard’s estimation method were comparable to the reference method for all particle morphologies within the surface area ratios of 3.31 and 0.19 for assumed GSDs 1.5 and 1.8, respectively, when the bulk material density of silver was used. The difference between the Maynard’s estimation method and surface area measured by the reference method for fractal-like agglomerates decreased from 79% to 23% when the measured effective particle density was used, while the difference for nearly spherical particles decreased from 30% to 24%. The results indicate that the use of particle density of agglomerates improves the accuracy of the Maynard’s estimation method and that an effective density should be taken into account, when known, when estimating aerosol surface area of nonspherical aerosol such as open agglomerates and fibrous particles.

Address correspondence to Bon Ki Ku, National Institute for Occupational Safety and Health (NIOSH), Centers for Disease Control and Prevention (CDC), 4676 Columbia Parkway, MS-R3, Cincinnati, Ohio 45226, USA. BKu@cdc.gov.

INTRODUCTION

Recent review articles and toxicology studies have indicated the potential occupational health risks associated with inhaling some types of nanoparticles and have suggested that evaluating exposures to such particles using aerosol surface area may be more appropriate under some circumstances (Oberdörster et al. 2005; Nel et al. 2006; Stoeger et al. 2006). Workplace emissions of engineered nanoparticles are widespread and exposures are likely to occur as the production of engineered nanomaterials increases [National Institute for Occupational Safety and Health (NIOSH) 2007, 2009). This widespread potential exposure leads to a need to develop and validate new methods of determining aerosol exposures in terms of surface area. Where aerosol surface area is not measured or known, methods that estimate workplace exposure by surface area from other metrics commonly monitored may be useful.

Two near real-time methods for estimating aerosol surface area using number and mass concentrations have been suggested for analyzing exposures to nanoparticles in the atmosphere and workplace (Woo et al. 2001; Maynard 2003). Maynard (2003) used particle number and mass concentration measurements to demonstrate that aerosol surface-area estimates are likely to be obtained within a factor of 4 of the actual surface area for a wide range of surface area concentrations. He pointed out that although the estimated errors are high, the method provides a means of estimating aerosol surface area exposure easily in the workplace where measurements of aerosol number and mass concentration are frequently made in parallel (Peters et al. 2006; Heitbrink et al. 2009; Evans et al. 2010). Recently, Park et al. (2009) showed that particle number and mass concentration measurements could be used to estimate aerosol surface area in residences with a correction factor of 2–6. Their paper reported that one source of error for the Maynard's method might be due to an assumed geometric standard deviation (GSD = 1.8), which can vary depending on actual particle size distributions. It is worth noting that in the Maynard method, particles with a known bulk material density are assumed. For nanoparticles with complex structures or nonspherical morphologies, e.g., open agglomerates and fibrous particles, it is anticipated that the actual density of agglomerates may be significantly different from the material density and that using the material density may upset the relationship between surface area and mass when the Maynard method is used. To quantitatively investigate how much the Maynard method depends on particle morphology, it is necessary to have known particle size distributions and controlled morphologies.

For this present study, the Maynard's estimation method was evaluated and compared with mobility based methods for agglomerates and compact particles using well-defined polydisperse aerosols with controlled morphologies and known particle densities. The main aim of the study was to quantitatively investigate the effect of agglomerate particle density on the Maynard's surface area estimation method. Polydisperse silver aerosol particles were generated by an aerosol generation facility developed by Ku and Maynard (2006). The particles generated had a range of morphologies with count median diameters (CMD) between 25 and 50 nm and GSD between 1.5 and 1.8. The density of particles with different morphologies was measured by tandem mobility mass analysis (Ku et al. 2006).

EXPERIMENTAL METHODS

Figure 1 shows the experimental setup for this study; its characteristics have previously been investigated by Ku and Maynard (2006). Briefly, the facility is capable of generating silver test aerosols with spherical and fractal-like morphologies in the size ranging from 15 nm to several hundred nanometers mobility diameter at number concentrations of the order of 10^3 to 10^4 particles/cm^3 for monodisperse aerosols and approximately 10^7 particles/cm^3 for polydisperse aerosols. Aerosol morphology is controlled using a sintering furnace at different temperatures ranging from room temperature (approximately 20°C) up to 900°C (near the melting point of 962°C for bulk silver).

The number size distributions of polydisperse aerosols generated at different sintering temperatures were measured using a scanning mobility particle sizer (SMPS, Model 3936, TSI, Inc.) together with a condensation particle counter (CPC, Model 3022a, TSI, Inc.). The SMPS was calibrated using standard monodisperse polystyrene latex (PSL) particles of diameters 20 and 100 nm (Duke Scientific Co.).

For aerosol mass measurements, an aerosol photometer (DustTrak, Aerosol Monitor Model 8520, TSI, Inc.) was used, together with filter media in parallel (0.6-μm pore size, Polyvic-BD [Polyvinyl Chloride], Millipore Corp.). Particles were sampled onto the filter for 1 h at a flow rate of 1 Lpm and then weighed using a microbalance (AT20, resolution 2 μg, Mettler-Toledo). The filters and the microbalance were stored in a controlled environment where relative humidity (RH) and temperature were controlled and remained about 30% RH and 22°C, respectively, when loading, unloading, and weighing the filters. The filter conditioning in the controlled environment reduced measurement errors considerably minimizing the presence of adsorbed water on the filter. Also, the filters were neutralized on Polonium strips for at least 10 s prior to weighing. The uncertainty on the mass data was expressed as the standard deviation of three measurements made for the DustTrak and as a detection limit of the filter (Vaughan et al. 1989) plus balance sensitivity for the filter.

To control particle morphology, sintering temperatures were varied between 20°C (room temperature) and 500°C. Transmission electron microscopy (TEM) samples were collected using a thermophoretic precipitator (Maynard 1995) or impactor-based electrostatic precipitator (Ku and Maynard 2005).

SURFACE-AREA MEASUREMENT METHODS

To quantitatively evaluate the Maynard's estimation method, reference surface areas were calculated on the basis of two different approaches for agglomerates and sintered compact particles, respectively.

Reference Surface Area Calculation of Agglomerates and Compact Particles

To calculate surface area of agglomerates, a method proposed by Lall and Friedlander (2006) was used. The method was based on estimation of surface area using mobility diameter of agglomerates. This method relates the number (N_p) and the radius (a) of primary particles that compose the agglomerates to the mobility diameter (d_m).

$$\frac{d_m}{C\,(d_{\mathrm{m}})}=\frac{c^* N_p a^2}{3\pi\lambda}, \quad [1]$$

where C is the slip correction factor, λ is the mean free path of the gas, and c^* is the dimensionless drag force for agglomerates (c^* = 6.62 for motion parallel to viscous flow of gas [Chan and Dahneke 1981]). Surface area can be obtained from Equation (1) by summing the surface areas of the primary particles in the agglomerate. This surface area was used as a reference surface area of nonsintered and partially sintered agglomerates.

To calculate surface area of sintered compact particles, an SMPS was used to give a reference aerosol surface area from the measured number size distribution. Previous studies showed that the mobility diameter of an agglomerate or spherical particle is nearly equal to the diameter of a sphere with the same projected surface area measured by TEM for monodisperse open silver agglomerates below 100 nm and for TiO_2 agglomerates below 400 nm (Rogak et al. 1993; Ku and Maynard 2005). On the basis of this fact, an SMPS size distribution could give an approximate estimation of surface area at least for compact sintered particles. The particle size range measured by the SMPS was from 15 to 680 nm. The assumptions were that particles were spherical and had a physical diameter equivalent to their mobility diameter. Therefore, the aerosol surface area was determined by a conversion of the appropriate number size distributions over the measured size range. In this study, the SMPS software was used to obtain aerosol surface area from the number size distributions.

Estimation of Aerosol Surface Area from Number and Mass Concentration Measurements

This method is based upon the approach reported by Maynard (2003; referred to as "Maynard's estimation method"). By assuming a lognormal aerosol size distribution with a specific GSD, number and mass concentration measurements can be used to estimate the surface area concentration associated with the distribution. According to Maynard (2003), if a unimodal lognormal particle size distribution is assumed, distribution function F can be expressed as

$$F(x_1, x_2, \ldots, x_m, d) \equiv N\Phi(\mathrm{CMD}, \sigma_{\mathrm{g}}, d), \quad [2]$$

where $x_1 = N$ (number concentration), x_2 = CMD, and $x_3 = \sigma_{\mathrm{g}}$ (GSD). Φ is the normalized lognormal function.

The difference between the expected values (N_{ex} is the expected total number concentration and m_{ex} is the expected mass concentration) and measured values (N_{meas} and m_{meas}) will be minimized when the following relation is met,

$$\frac{N_{\mathrm{ex}}}{m_{\mathrm{ex}}}=\frac{N_{\mathrm{meas}}}{m_{\mathrm{meas}}}, \quad [3]$$

and, eventually, the following equation is obtained,

$$\frac{N}{m}=\frac{N_{\text{meas}}\int_{d_{2,\min}}^{d_{2,\max}}\Phi(\text{MMD},\sigma_{\text{g}},d)dd}{m_{\text{meas}}\int_{d_{1,\min}}^{d_{1,\max}}\Phi(\text{CMD},\sigma_{\text{g}},d)dd}, \quad [4]$$

where ρ is the particle density, d_{ma} is the diameter of average mass and $\text{d}_{i,\min}$ and $\text{d}_{i,\max}$ (index i = 1 for particle count and i = 2 for particle mass) represent the size range over which the measurement instrument operates. The additional relationships $m=N\rho(\pi \text{d}_{\text{ma}}^3/6)$ and $d_{\text{ma}} = \text{CMDe}^{1.5\ln^2\sigma_{\text{g}}}$ can be used to evaluate N/m as a function of assumed values of ρ and σ_{g}, as shown in Equation (5).

$$\frac{N}{m}=\frac{6}{\pi\rho}(\text{CMDe}^{1.5\ln^2\sigma_{\text{g}}})^{-3} \quad [5]$$

Thus, if σ_{g} is fixed, Equations (4) and (5) can be solved iteratively by changing CMD to obtain N/m. Once N/m is determined, CMD and N are determined. In this study, number (N_{meas}) concentration and mass concentration (m_{meas}) were measured using the SMPS and CPC, and DustTrak and filter media, respectively.

Aerosol surface area concentration from two independent measurements of particle number and mass concentrations can be calculated as follows:

$$S=N\pi d_{\text{s}}^2, \quad [6]$$

where the d_{s} is the diameter of average surface and $d_{\text{s}} = \text{CMDe}^{\ln^2\sigma_{\text{g}}}$.

It is worth noting that in Equation (5) a particle density is required, and for this, Maynard (2003) assumed particles with a bulk material density. This assumption is reasonable for compact particles, but the assumption may not be applied to nonspherical particles such as open agglomerates, and thus it is necessary to use an actual particle density for estimating the aerosol surface area by the Maynard's estimation method. To investigate the effect of particle density on the Maynard's estimation method, another experiment was performed to measure particle densities of silver agglomerates used in this study. The related experimental setup is shown in Figure 2.

Differential mobility analyzer (DMA)-classified monodisperse agglomerates were provided into an aerosol particle mass analyzer (APM, Model 3600, Kanomax, Inc.) to measure mean particle mass. Briefly, the APM consists of two concentric cylinders that rotate together at a controlled rate. The outer cylinder (52 mm in radius) is electrically grounded, and a classifying voltage is applied to the inner cylinder (50 mm in radius). Charged particles introduced axially into the small annular gap experience centrifugal and electrostatic forces, which act in opposite directions. The concentration of particles downstream from the APM is measured as the classifying voltage is varied as shown in Figure 3. The concentrations attain a peak value at the voltage where the centrifugal and electrostatic forces are balanced (McMurry et al. 2002; Ku et al. 2006; Maynard et al. 2007). Further details on the APM are described in previous papers (Ehara et al. 1996; McMurry et al. 2002).

Several definitions for effective density of agglomerates have been well discussed by DeCarlo et al. (2004). The effective density measured in our study was based on particle mobility diameter and mass measured, which was defined as the particle mass divided by the particle volume based on mobility diameter, in a similar way as shown in the previous studies (McMurry et al. 2002; Ku et al. 2006). The densities of the monodisperse agglomerates with mobility diameters ranging from 50 to 400 nm were obtained. The uncertainty for mass or density measurement using the APM was measured for standard PSL particles and was found to be within 6%.

RESULTS

A Comparison of Maynard's Estimation Method with Reference Methods

Figure 4 shows typical size distributions of polydisperse particles measured by the SMPS at different sintering temperatures. Figure 5 shows morphologies of particles at the corresponding temperatures. Table 1 summarizes statistics for the size distributions in Figure 4 such as total number concentration, CMD, and GSD particles. Particles with no sintering have CMD of about 45 nm and GSD of about 1.8 and the CMD and GSD decreases down to 27 nm and 1.5, respectively, as sintering temperature increases. Nonsintered particles have fractal-like morphology of agglomerates with open structure as shown in Figure 5a, while the particles sintered at 500°C show smaller CMD and GSD with compact and nearly spherical shapes.

CMDs and GSDs obtained from TEM image analysis using ImageJ analyses are summarized in Table 2. Figure 6 represents a typical size distribution of particles from TEM analysis and related image processed pictures. The diameters extracted from TEM image analysis are projected area diameters. TEM analysis confirms the tendency for CMD to decrease with increasing sintering temperature even though all the CMDs from TEM are smaller than the CMDs measured by the SMPS probably due to lower collection efficiency of larger particles on TEM grid. It is worth noting that for particles sintered at 500°C as shown in Figure 5d, the particles with sizes less than 100 nm are nearly spherical and the number concentration of the particles larger than 100 nm is very low as shown in Figure 4.

Table 3 shows CMDs estimated by the Maynard's estimation method using number and mass concentrations, assuming GSDs. The estimated CMDs are larger than CMDs measured by the SMPS for GSD = 1.5, while they are smaller than those for GSD = 1.8. It is expected that a CMD is smaller for a larger GSD because the total aerosol number and mass concentrations are fixed for both of the assumed GSDs. In other words, as the GSD increases, the CMD decreases to keep aerosol number and mass concentrations constant.

Figure 7 shows total aerosol mass concentrations at the different sintering temperatures used for the Maynard's estimation method. The particle gravimetric mass collected by filter was sampled at an aerosol flow rate of 1 Lpm for 1 h and used to derive aerosol mass concentration. The error bars on the data in Figure 7 are expressed as a standard deviation of three measurements made for the DustTrak and as a detection limit for the filters, which is defined as three times the standard deviation of a blank sample result (Vaughan et al. 1989)

plus balance sensitivity. It was found that the particle mass measured at each sintering temperature was in the order of 100 μg, which is well above the resolution of the balance.

Figure 8 shows estimations of aerosol surface area from number and mass concentration measurements using assumed GSDs. For lower assumed GSD (1.5), the surface area estimates are larger than the calculated reference surface area by a factor of 3 for the filter, while they are comparable with the calculated reference data for the DustTrak within the ratio of estimated surface area to calculated surface area of 0.30–1.55. For larger assumed GSD (1.8), the estimates showed fair agreement with the calculated data, where differences are up to the ratio of 0.21–0.70 for filter and 0.19–1.01 for DustTrak. The correlation between calculated surface area and estimated surface area was also examined. Estimated surface area based on filter measurements shows good correlations for the two estimates of GSDs (1.5 and 1.8). However, the surface area based on the DustTrak data resulted in poor correlations, for which the correlation parameter R^2 corresponds to 0.06 and 0.05 for GSDs of 1.5 and 1.8, respectively. It may be reasonable to assume that the mass of the agglomerates measured by the filter media at 20°C is more reliable than the one measured by the DustTrak under the same condition because some errors associated with the particle-loaded filter weighing such as humidity and electrostatics effects were minimized when the particle mass was measured in the controlled environment. It is reported that the gravimetric uncertainty is mostly due to weighing procedure and initial and final mass filter conditioning (Buonanno et al. 2011). Therefore, it is believed that our gravimetric mass measurement in the controlled environment is reliable. If we do not consider the datum of the DustTrak at 20°C because the mass measured by the DustTrak is well below the mass by filter, each linear fit for the assumed GSD 1.5 and 1.8 gives relatively reasonable correlations for which R^2 is 0.8155 and 0.8301, respectively (not shown in Figure 8).

All the surface areas estimated by the method are summarized in Table 4. For the assumed GSDs (1.5 and 1.8), the surface area from the Maynard's estimation method lies within a factor of 0.19–1.01 or 81% of values derived from the reference surface area for the GSD = 1.8, and it deviates from the SMPS data by a factor of 3.31 or 231% for the GSD = 1.5. These data mean that the method overestimates the surface area for GSD = 1.5, lower than actual GSDs and underestimates the surface area for GSD = 1.8 by a factor of about 5, indicating that the error of the Maynard's estimation method for GSD = 1.8 is worse than that for GSD = 1.5. Maynard (2003) showed that assuming the higher GSD reduced the error of the estimate considerably and that most measured size distributions have a GSD closer to 1.8. Also, Park et al. (2009) reported that the Maynard's estimation method is very dependent on the assumed GSD. Considering that the GSDs measured by the SMPS are in the range from 1.51 to 1.79, as shown in Table 1, the average of the SMPS GSDs (1.66) seems to provide reasonable agreement across the entire range. It is worth noting that the Maynard's estimations are in better agreement to the mobility based measurements for particles with compact (300°C) and nearly spherical shapes (500°C) than for agglomerated particles (200°C and no sintering) for both filter and DustTrak with GSD = 1.8. On the basis of the data in Table 4, for the case of filter and DustTrak with GSD = 1.8, the Maynard's estimation method gives a better estimation of the surface area within a factor of 0.63–1.01, especially for nearly spherical particles, while it seems that a reasonable estimation of

aerosol surface area for all particle shapes may occur somewhere between GSD = 1.5 and 1.8.

The Effect of Particle Density on Maynard's Estimation Method

The agglomerate particle sizes in this study ranged from 50 to 400 nm in diameter. The corresponding density was found to be in the range from 0.44 to 2.24 g cm^{-3}. The density of the agglomerates decreased as the size of the agglomerates increased, which means that the agglomerates have more open structure as size increases. Given that the bulk density of a spherical silver particle is 10.5 g cm^{-3}, the densities measured in the size range are significantly low. The estimates of surface area were obtained for DustTrak and filter with the assumed GSD = 1.8 using an effective density of the agglomerates and are shown in Table 5. The results clearly show that the error of estimates compared to the reference surface area calculated by the model decreases as the particle density decreases for both DustTrak and filter. For the filter case, the error decreased first and then increased as the density decreased. This particular aerosol seems to have an effective density to minimize the error of its estimates. The minimum error or maximum accuracy of the method can be obtained when the effective density of agglomerates is 0.95 g cm^{-3}, which corresponds to the density of agglomerates with 200 nm. The contribution to surface area of agglomerates larger than modal diameter (approximately 50 nm) for the case of nonsintered particles is expected to be significant. It is therefore reasonable to assume that a representative density of the agglomerates in the whole size range will be the one for agglomerates at a modal diameter or mean diameter of a surface area-weighted size distribution. The surface area-weighted size distribution obtained from the number size distribution for nonsintered particles in Figure 4 was found to have a surface mean diameter of about 116 nm, which is between 100 and 150 nm among the particle sizes measured for the effective densities. If we use an effective density of 1.79 or 1.29 g cm^{-3} for the surface area estimate, which corresponds to 100 and 150 nm, respectively, the estimate shows better agreement with the reference value within 23% compared with the estimate within 79% when the bulk density of silver was used. The results clearly show that the use of effective density of agglomerates improves the accuracy of the Maynard's estimation method.

Table 6 shows surface area estimation from total number and mass concentrations using measured effective particle densities for nearly spherical particles sintered at 500°C, assuming GSD = 1.8. The density of the nearly spherical silver particles decreases from 8.61 to 3.55 g cm^{-3} as particle size increases from 50 to 150 nm. It is worth noting that particles in the size range of 50 to 100 nm have a similar density to one another and also have a density close to the bulk material density of silver. The difference between estimated surface area and reference surface area measured by the SMPS slightly decreases as particle density decreases from 8.61 to 5.39 g cm^{-3} and then increases significantly as particle density decreases from 5.39 to 1 g cm^{-3}. As can be seen in Figure 4, most of the particles sintered at 500°C have sizes below 150 nm, indicating that densities of the majority particles are in the range from 5 to 10.5 depending on the degree of spherical shape, as shown in Figure 5d. This fact was confirmed by the numerical integration of the measured particle density with the number concentration, which showed that the average density of the particles is 8.71 g cm^{-3}. The data from Tables 4 and 6 indicate that the Maynard's estimation method works

well for nearly spherical particles with the particle material density, in our case, silver density.

Figure 9 shows deviation of the estimated surface area of agglomerates and nearly spherical particles from reference surface area as a function of particle density used for the Maynard's estimation method. The clear difference between agglomerates and spherical particles is that the deviation of the estimated surface area of agglomerates decreases as particle density decreases down to 1.0 g cm^{-3}, while the deviation for spherical particles increases as particle density decreases. The minimum deviation, i.e., around 0%, occurs with particle density between 1.0 and 0.8 g cm^{-3} for agglomerates, while it occurs with particle density of about 6.0 g cm^{-3} for nearly spherical particles. The reason the use of effective particle density improves the accuracy of the Maynard's estimation method is that agglomerate particles have a density lower than their material density, as shown in Table 5. There are fewer number of agglomerate particles for a given particle volume than for compact spherical particles, which translates to less mass per unit volume (i.e., lower particle density). It was observed that the density of aggregates decreases as the mobility diameter increases. This is expected for a fractal-like particle. The actual volume of material in an agglomerate with a fractal dimension smaller than 2 can be approximated by a disk one primary particle thick, neglecting overlap. One would then expect that the density should decrease more or less as the inverse of the diameter. For measured total number and mass concentrations, this lower particle density results in an increased estimated surface area and decreased deviation.

DISCUSSION

Particle Density Influence on Maynard's Estimation Method

In the previous section, it was shown that the effective particle density affects the accuracy of the Maynard's estimation method. Because the effective density can span up to a range of about 24 (e.g., from 0.44 to 10.5 g cm^{-3}) for agglomerate particles, the difference between the estimated surface area and reference surface area was significant when the material density was used. On the other hand, the Maynard's method was found to work well for nearly compact spherical particles assuming the material particle density. According to the measurement of effective density of the particles sintered at 500°C, most of particles with sizes smaller than 100 nm were found to have density of about 8.5 g cm^{-3}, which is 19% difference from the material density of silver. This fact justifies using the material density to estimate surface area of compact particles from the Maynard's method.

Uncertainty of Aerosol Photometer

The advantage of the Maynard's estimation method is that it provides a means of estimating aerosol surface area exposure easily in the workplace where measurements of aerosol number and mass concentration are frequently made in parallel in real time. The aerosol photometer is used to measure aerosol mass concentration in the workplace and provides important insights into how exposures may occur (Demou et al. 2008; Evans et al. 2010). However, in our study, the aerosol photometer (DustTrak) measuring aerosol mass had the lowest response to fractal-like agglomerate particles compared with the filter measurements

while it responded fairly to particles with relatively compact and spherical shapes. The difference between the aerosol photometer and filter measurements was found to be in the range of 23% to −83% (corresponding to a factor of 1.23–0.17). In our study, a calibration factor for the photometer was not measured but was used with its default factory calibration factor (defined as a ratio of gravimetric mass concentration to photometer mass concentration) for A1 test dust (Arizona Test Dust). On the basis of our mass measurements using filters, the calibration factors for silver particles can be calculated as 6.02, 0.82, 1.32, and 4.63, respectively, with increasing sintering temperature. The aerosol photometer response depends on particle size distribution, shape, the refractive index of particles, and the bulk material density of particles (Wang et al. 2009). Our calibration factors indicate that particle shapes and size distributions at different sintering temperatures affect the aerosol photometer. It is worth noting that there is the largest discrepancy between the DustTrak and filter media at 20°C as shown in Figure 7. The lower mass directly affects the Maynard's estimation method by increasing the error of estimates. If the mass measured by the filter is used at 20°C instead of the DustTrak-measured mass, the errors were reduced from 81% to 65% for GSD = 1.8 and from 70% to 48% for GSD = 1.5. This result shows that the lower mass detection can increase the error by about 16%–22%. It is also hypothesized that fractal-like agglomerates with small primary particles for other materials such as diesel particulate matter (DPM; most diesel aerosol particles are typically carbonaceous soot agglomerates formed directly by combustion in the accumulation mode; Kittelson 1998) may be detected less by light-scattering sensors such as the photometer in a similar way. Thus, photometer use should be exercised with caution for fractal-like agglomerates with small primary particles.

Implication of the Maynard's Estimation Method for Monitoring Aerosol Surface Area Exposures in the Workplace

One issue for use of the Maynard's estimation method is that the assumed particle density, i.e., material density of the particle, causes a significant error in estimation of the particle surface area for silver agglomerates approximately 55% higher than the actual particle density. The error could be even more drastic for complex aerosols with high dynamic shape factors, such as carbon nanotube agglomerates. It is not expected that an aerosol generated in workplace will have spherical shape, particularly nanoparticles. For example, the aerosols generated from processes involving one dominant generation mechanism, such as welding, smelting, and powder handling, may have a single mode distribution and may also be agglomerates, not single spherical particles (Zimmer et al. 2002; Evans et al. 2010). In this case, the actual particle density will be very different from the material density of the particle. Thus, it is important to estimate the effective particle density when the Maynard's estimation method is used in the workplace to measure aerosol surface area. Normally, when particles become agglomerated within themselves, the effective density of the particles is lower than the material density of the particles because agglomerates have relatively large open voids compared with nonagglomerated particles. This fact was confirmed for silver agglomerates in our study and for carbon nanofibers (CNFs) in the work of Ku et al. (2006) where it was shown that the effective density of CNFs aerosolized by a vortex shaker decreased as mobility diameter of the CNFs increased. Therefore, an effective particle

density could be estimated as a density lower than the material density, although the actual density strongly depends on agglomeration state of particles.

Another issue of the Maynard's estimation method is that the particle surface physical characteristics, such as particle roughness and pores, and their contribution to surface area are not captured by the method. Particle roughness may increase particle surface area (Ono-Ogasawara and Kohyama 1999) and particle pores may affect particle surface area somehow. The third issue for use of the method occurs in the occupational environment, where different types of aerosols come from a variety of sources. This situation makes surface area measurement more challenging for all instruments and methods including the Maynard's estimation method because we need to selectively measure the particles of interest from other particles. This contamination issue has been addressed in recent studies (Seipenbusch et al. 2008; Evans et al. 2010). Evans et al. (2010) reported that all particles observed as a transient concentration elevation in response to a dryer dump event were not due to CNFs at a facility that manufactures and processes CNFs. They found that the transient increase in particle number was not due to CNFs, but rather, condensable ultrafine particles emitted. Seipenbusch et al. (2008) investigated the evolution in time of a nanoparticle aerosol released into a simulated workplace environment for different starting scenarios. They showed that the nanoparticles are still chemically present in the aerosol after becoming attached to background particles, thus remaining airborne while being invisible in the nanometer size range. On the basis of these studies, without physical information such as particle morphology and agglomeration state about workplace aerosols emitted, the Maynard's estimation method may cause significant deviation of estimated surface area of the particles under investigation from actual surface area. McMurry and colleagues (2002) applied tandem mobility mass analysis to urban atmospheric aerosols to measure effective densities of the particles. Following their approach, particle effective density in the workplace could be determined in a similar way even though highly specialized instruments such as SMPS and APM are needed.

CONCLUSIONS

The estimates from the total number and mass concentration measurements were comparable to the reference methods for all morphologies of silver agglomerates within the surface area ratios of 3.31 and 0.19 for assumed GSDs 1.5 and 1.8, respectively, when the material density of silver was used. The difference between the estimate and surface area measured by the reference method for fractal-like agglomerates decreased from 79% to 23% when the measured effective particle density was used while the difference for nearly spherical particles decreased from 30% to 24%. The number and mass estimates correlated well with the two reference calculations when gravimetric mass was used, depending on the assumed value of GSD used for CMDs less than 100 nm. The results clearly show that the use of actual agglomerate density improves the accuracy of the Maynard's estimation method and that the use of particle density of agglomerates should be taken into account, when known, when estimating surface area of nonspherical aerosol such as open agglomerates and fibrous particles. Particle effective density in the workplace could be determined using tandem mobility mass analysis even though highly specialized instruments such as SMPS and APM are needed.

Acknowledgments

The authors would like to thank Dr. Andrew Maynard, School of Public Health at the University of Michigan; Dr. Aleks Stefaniak, Division of Respiratory Disease Studies (DRDS)/National Institute for Occupational Safety and Health (NIOSH) in Morgantown, WV, for his invaluable comments and suggestions on this work; and Ellen Galloway for editorial assistance. This work was funded by the NIOSH through the Nanotechnology Research Center (NTRC) program (project CAN 927ZBCL).

References

Buonanno G, Dell'Isola M, Stabile L, Viola A. Critical Aspects of the Uncertainty Budget in the Gravimetric PM Measurements. Measurement. 2011; 44:139–147.

Chan P, Dahneke B. Free-Molecular Drag on Straight Chains of Uniform Spheres. J Appl Phys. 1981; 52:3106–3110.

DeCarlo PE, Slowik JG, Worsnop DR, Davidovits P, Jimenez JL. Particle Morphology and Density Characterization by Combined Mobility and Aerodynamic Diameter Measurements. Part 1: Theory. Aerosol Sci Technol. 2004; 38:1185–1204.

Demou E, Peter P, Hellweg S. Exposure to Manufactured Nanostructured Particles in an Industrial Pilot Plant. Ann Occup Hyg. 2008; 52(8):695–706. [PubMed: 18931382]

Ehara K, Hagwood C, Coakley KJ. Novel Method to Classify Aerosol Particles According to Their Mass-to-Charge Ratio-Aerosol Particle Mass Analyzer. J Aerosol Sci. 1996; 27:217–234.

Evans DE, Ku BK, Birch ME, Dunn KH. Aerosol Monitoring During Carbon Nanofiber Production: Mobile Direct-Reading Sampling. Ann Occup Hyg. 2010; 52:9–21. [PubMed: 18056626]

Heitbrink WA, Evans DE, Ku BK, Maynard AD, Slavin TJ, Peters TM. Relationships Among Particle Number, Surface Area, and Respirable Mass Concentrations in Automotive Engine Manufacturing. J Occup Environ Hyg. 2009; 6:19–31. [PubMed: 18982535]

Kittelson DB. Engines and Nanoparticles: A Review. J Aerosol Sci. 1998; 29:575.

Ku BK, Emery MS, Maynard AD, Stolzenburg MR, McMurry PH. In Situ Structure Characterization of Airborne Carbon Nanofibres by a Tandem Mobility-Mass Analysis. Nanotechnology. 2006; 17:3613–3621. [PubMed: 19661613]

Ku BK, Maynard AD. Comparing Aerosol Surface-Area Measurements of Monodisperse Ultrafine Silver Agglomerates by Mobility Analysis, Transmission Electron Microscopy and Diffusion Charging. J Aerosol Sci. 2005; 36:1108–1124.

Ku BK, Maynard AD. Generation and Investigation of Airborne Silver Nanoparticles with Specific Size and Morphology by Homogeneous Nucleation, Coagulation and Sintering. J Aerosol Sci. 2006; 37:452–470.

Lall AA, Friedlander SK. On-Line Measurement of Ultrafine Aggregate Surface Area and Volume Distributions by Electrical Mobility Analysis: 1. Theoretical Analysis. J Aerosol Sci. 2006; 37:260–271.

Maynard AD. The Development of a New Thermophoretic Precipitator for Scanning Transmission Electron Microscope Analysis of Ultrafine Aerosol Particles. Aerosol Sci Technol. 1995; 23:521–533.

Maynard AD. Estimating Aerosol Surface Area from Number and Mass Concentration Measurements. Ann Occup Hyg. 2003; 47:123–144. [PubMed: 12581997]

Maynard AD, Ku BK, Emery M, Stolzenburg M, McMurry PH. Measuring Particle Size-Dependent Physicochemical Structure in Airborne Single Walled Carbon Nanotube Agglomerates. J Nanoparticle Res. 2007; 9:85–92.

McMurry PH, Wang X, Park K, Ehara K. The Relationship Between Mass and Mobility for Atmospheric Particles: A New Technique for Measuring Particle Density. Aerosol Sci Technol. 2002; 36:227–238.

Nel A, Xia T, Mädler L, Li N. Toxic Potential of Materials at the Nanolevel. Science. 2006; 311:622–627. [PubMed: 16456071]

NIOSH. Progress Toward Safe Nanotechnology in the Workplace: A Report from the NIOSH Nanotechnology Research Center. DHHS (NIOSH); 2007. Publication No. 2007-123]. http://www.cdc.gov/niosh/docs/2007-123/pdfs/2007-123.pdf

NIOSH. Approaches to Safe Nanotechnology: Managing the Health and Safety Concerns Associated with Engineered Nanomaterials. DHHS (NIOSH); 2009. Publication No. 2009-125http://www.cdc.gov/niosh/docs/2009-125/pdfs/2009-125.pdf

Oberdörster G, Maynard A, Donaldson K, Castranova V, Fitzpatrick J, Ausman K, et al. Principles for Characterizing the Potential Human Health Effects from Exposure to Nanomaterials: Elements of a Screening Strategy. Part Fiber Toxicol. 2005; 2:8.

Ono-Ogasawara M, Kohyama N. Evaluation of Surface Roughness of Fibrous Minerals by Comparison of BET Surface Area and Calculated One. Ann Occup Hyg. 1999; 43:505–511.

Park JY, Raynor PC, Maynard AD, Eberly LE, Ramachandran G. Comparison of Two Estimation Methods for Surface Area Concentration Using Number Concentration and Mass Concentration of Combustion-Related Ultrafine Particles. Atmos Environ. 2009; 43:502–509.

Peters TM, Heitbrink WA, Evans DE, Slavin TJ, Maynard AD. The Mapping of Fine and Ultrafine Particle Concentrations in an Engine Machining and Assembly Facility. Ann Occup Hyg. 2006; 50:249–257. [PubMed: 16361396]

Rogak SN, Flagan RC, Nguyen HV. The Mobility and Structure of Aerosol Agglomerates. Aerosol Sci Technol. 1993; 18:25–47.

Seipenbusch M, Binder A, Kasper G. Temporal Evolution of Nanoparticle Aerosols in Workplace Exposure. Ann Occup Hyg. 2008; 52:707–716. [PubMed: 18927101]

Stoeger T, Reinhard C, Takenaka S, Schroeppel A, Karg E, Ritter B, et al. Instillation of Six Different Ultrafine Carbon Particles Indicates a Surface Area Threshold Dose for Acute Lung Inflammation in Mice. Environ Health Perspect. 2006; 114:328–333. [PubMed: 16507453]

Vaughan NP, Milligan BD, Ogden TL. Filter Weighing Reproducibility and the Gravimetric Detection Limit. Ann Occup Hyg. 1989; 33:331–337.

Wang X, Chancellor G, Evenstad J, Farnsworth JE, Hase A, Olson GM, et al. A Novel Optical Instrument for Estimating Size Segregated Aerosol Mass Concentration in Real Time. Aerosol Sci Technol. 2009; 43(9):939–950.

Woo KS, Chen DR, Pui DYH, Wilson WE. Use of Continuous Measurements of Integral Aerosol Parameters to Estimate Particle Surface Area. Aerosol Sci Technol. 2001; 34:57–65.

Zimmer AT, Baron PA, Biswas P. The Influence of Operating Parameters on Number-Weighted Aerosol Size Distribution Generated from a Gas Metal Arc Welding Process. J Aerosol Sci. 2002; 33:519–531.

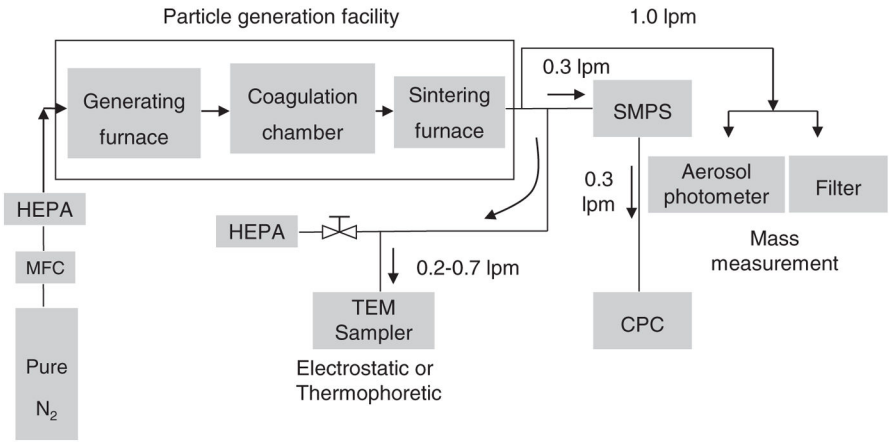

FIG. 1.

Experimental setup (MFC, mass flow controller; HEPA, high-efficiency particulate air filter; SMPS, scanning mobility particle sizer; CPC, condensation particle counter; TEM, transmission electron microscopy).

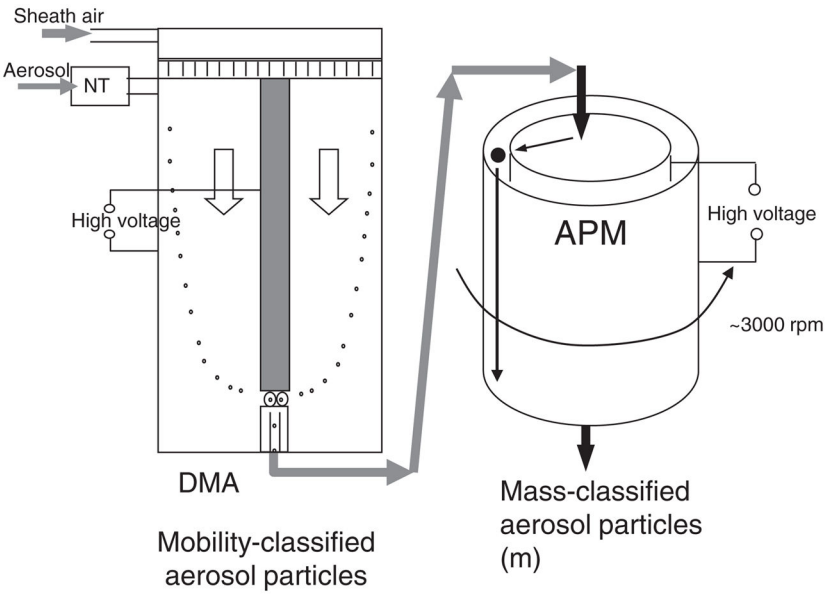

FIG. 2.

Schematic diagram for measuring an effective density of single mobility size particles by a tandem mobility mass analysis (DMA: differential mobility analyzer; APM: aerosol particle mass analyzer; NT: neutralizer). Adapted from Ku et al. (2006).

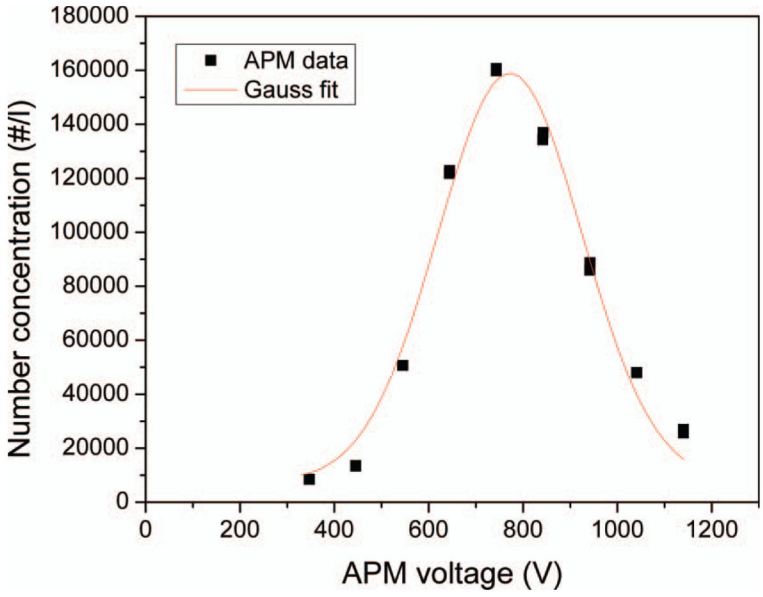

FIG. 3.

Typical number concentration as a function of APM voltage for particles classified by the APM at a fixed rotating speed. The peak voltage corresponds to mean mass of the classified particles. (Color figure available online).

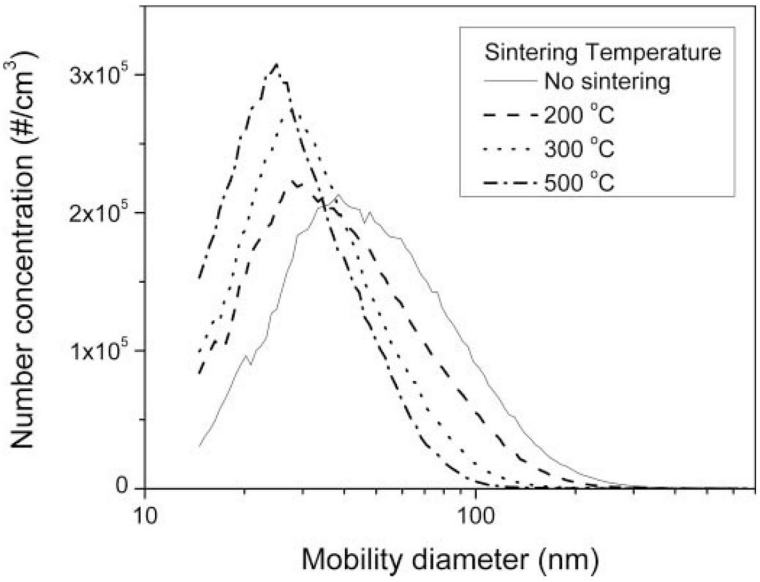

FIG. 4.

Typical size distributions measured by SMPS at different sintering temperatures (without sintering and with sintering at 500°C shown).

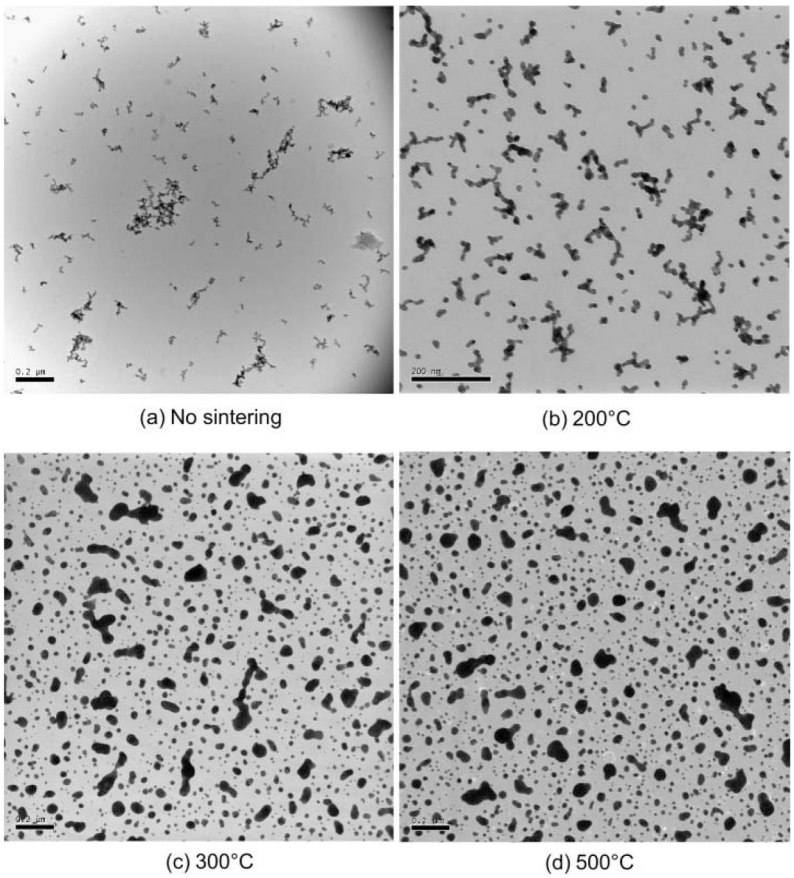

FIG. 5.
TEM images of polydisperse aerosols at different sintering temperatures.

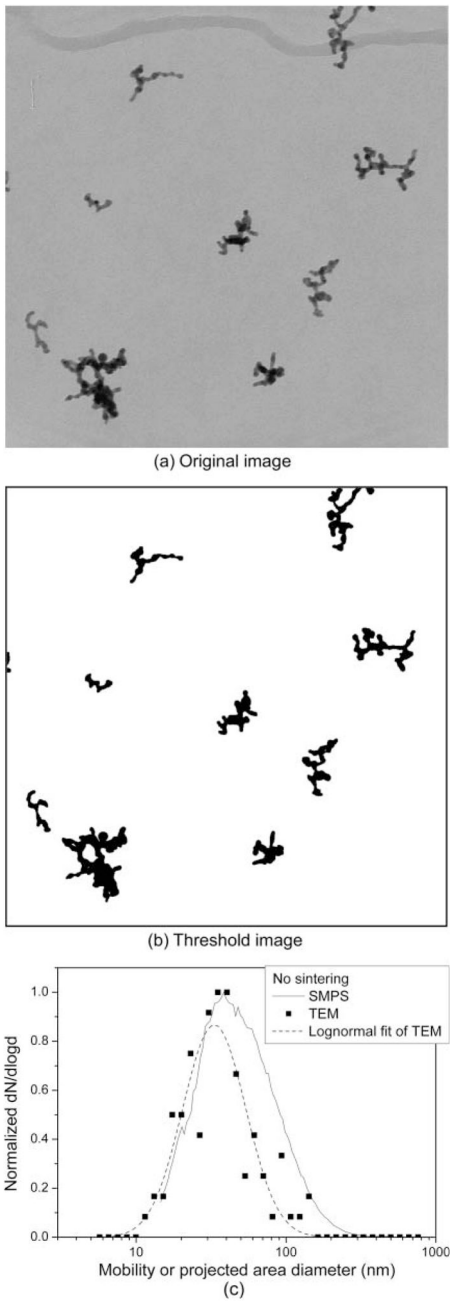

FIG. 6.

TEM images (a) before and (b) after image processing by threshold for no sintering for particles sampled by a thermophoretic precipitator. (c) Normalized number size distributions measured from SMPS and TEM data for the particles.

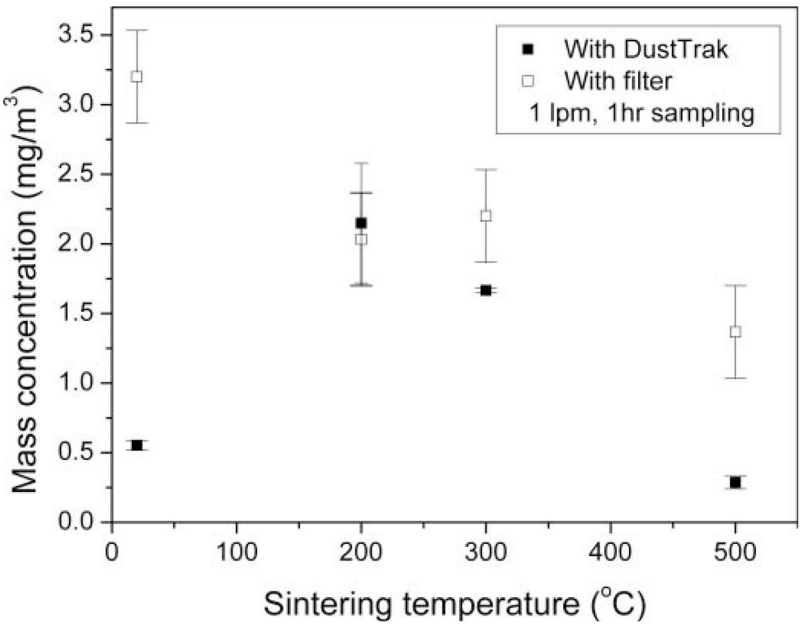

FIG. 7.

Comparison of aerosol total mass concentrations measured by the DustTrak and filter media at different sintering temperatures. The error bar on the data was expressed as the standard deviation of three measurements made for the DustTrak and as a detection limit of the filter (Vaughan et al. 1989) plus balance sensitivity for the filter. Notice the larger difference between two data at 20°C (no sintering), which indicates that the DustTrak appears not to detect fractal-like particles.

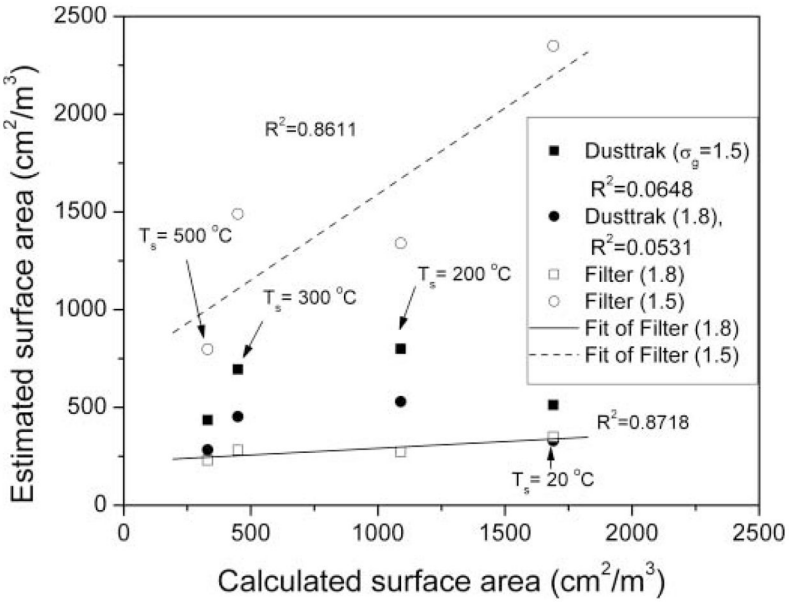

FIG. 8.

Estimation of aerosol surface-area from number and mass concentration measurements, assuming geometric standard deviation (σ_g) is 1.5 and 1.8 and particle density is 10.5 g cm^{-3}. Number concentration was taken from the size distribution measured with the SMPS and mass concentration measured using a DustTrak (TSI, Inc.) and filter media. Calculated surface areas for agglomerates at 20°C and 200°C and sintered particles at 300°C and 500°C were obtained, respectively, by the method by Lall and Friedlander (2006) and numerically integrating the surface area lognormal distribution over the measured size range of SMPS, assuming spherical particles. Also, shown is correlation between calculated surface area and number-mass estimate surface area. Note that filter samples show good correlations, but DustTrak data show poor correlations.

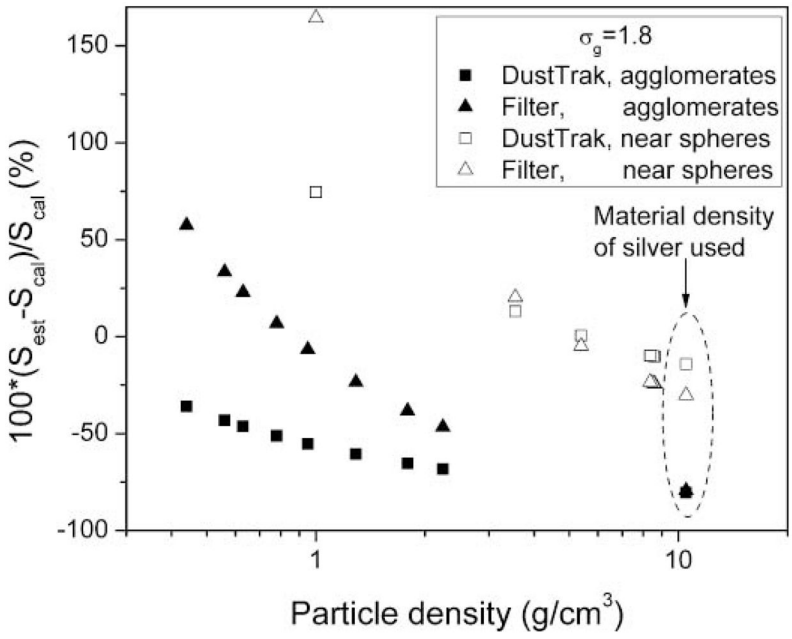

FIG. 9.

Difference between estimated surface area and calculated surface area as a function of particle density for filter and DustTrak data. S_{est} is estimated surface area and S_{cal} is surface area calculated by either the method for agglomerates (Lall and Friedlander 2006) or the SMPS for nearly spherical particles.

TABLE 1

Statistics of number distributions measured by SMPS at different sintering temperatures

Sintering temperature (°C)	Number concentration (cm^{-3})	CMD[a] (nm)	GSD[b]	Diameter of average mass (nm)
20	8.68E+06	45.2	1.79	75.2
200	8.54E+06	35.7	1.74	56.6
300	8.24E+06	30.5	1.58	41.7
500	8.41E+06	26.7	1.51	34.4

[a] CMD means count median diameter.

[b] GSD means geometric standard deviation.

TABLE 2

Statistics of number and surface area distributions measured by SMPS and TEM

Number	**SMPS**		**TEM (TP)**[a]		**TEM (EP)**[b]	
Sintering temperature (°C)	**CMD**	σ_g	**CMD**	σ_g	**CMD**	σ_g
20	45.2	1.79	33.2	1.62	—	—
200	35.7	1.74	21.2	1.86	17.6	1.64
300	30.5	1.58	18.0	1.68	15.8	2.22
500	26.7	1.51	—	—	24.8	2.69

[a] TP means thermophoretic sampling.

[b] EP means electrostatic precipitator sampling.

TABLE 3

Count median diameters estimated by Maynard's method using number and mass concentrations, assuming GSD = 1.5 and GSD = 1.8

			GSD = 1.5	GSD = 1.8
	Sintering temperature (°C)	**CMD (measured)**	**CMD (estimated)**	**CMD (estimated)**
F[a]	20 (no sintering)	45.2	79.4	22.0
F	200	35.7	60.4	17.9
F	300	30.5	64.3	18.8
F	500	26.7	46.6	14.3
D	20 (no sintering)	45.2	37.1	21.0
D	200	35.7	46.7	29.7
D	300	30.5	43.9	27.2
D	500	26.7	34.5	18.6

[a] F stands for filter and D for DustTrak (TSI, Inc.).

TABLE 4

Estimation of surface area from total number and mass concentrations, assuming GSD = 1.5 and GSD = 1.8

	Sintering temperature (°C)	Reference surface area S_{cal} (cm^2 m^{-3})	GSD = 1.5 Estimated surface area S_{est} (cm^2 m^{-3})	SR[d] (S_{est}/S_{cal})	%ΔS = 100* (S_{est} – S_{cal})/ S_{cal}	GSD = 1.8 Estimated surface area S_{est} (cm^2 m^{-3})	SR (S_{est}/S_{cal})	%ΔS = 100* (S_{est} – S_{cal})/ S_{cal}
F[a]	20 (no sintering)	1.69E+03 [b]	2.35E+03	1.39	39	3.50E+02	0.21	−79
F	200	1.09E+03 [b]	1.34E+03	1.23	23	2.73E+02	0.25	−75
F	300	4.49E+02 [c]	1.49E+03	3.31	231	2.82E+02	0.63	−37
F	500	3.30E+02 [c]	7.98E+02	2.42	142	2.30E+02	0.70	−30
D	20 (no sintering)	1.69E+03 [b]	5.13E+02	0.30	−70	3.29E+02	0.19	−81
D	200	1.09E+03 [b]	8.00E+02	0.73	−27	5.30E+02	0.49	−51
D	300	4.49E+02 [c]	6.95E+02	1.55	55	4.53E+02	1.01	1
D	500	3.30E+02 [c]	4.36E+02	1.32	32	2.83E+02	0.86	−14

[a] F stands for filter and D for DustTrak (TSI, Inc.).

[b] Obtained by a method proposed by Lall and Friedlander (2006) for nonsintered and partially sintered agglomerates.

[c] Obtained from the scanning mobility particle sizer (SMPS) for sintered compact particles.

[d] SR means a ratio of estimated surface area to reference surface area.

TABLE 5

Estimation of surface area from total number and mass concentrations using measured effective particle densities for agglomerates (nonsintered particles), assuming GSD = 1.8

Diameter[a] (nm)	Density[b] (g cm^{-3})	Reference surface area S_{cal} (cm^2 m^{-3})	DustTrak, GSD = 1.8 estimated surface area S_{est} (cm^2 m^{-3})	SR[c] (S_{est}/S_{cal})	%$\Delta S = 100^* (S_{est} - S_{cal})/S_{cal}$	Filter, GSD = 1.8 estimated surface area S_{est} (cm^2 m^{-3})	SR (S_{est}/S_{cal})	%$\Delta S = 100^* (S_{est} - S_{cal})/S_{cal}$
50	2.24	1.69E+03	5.35E+02	0.32	−68	9.02E+02	0.53	−47
100	1.79	1.69E+03	5.83E+02	0.34	−66	1.04E+03	0.62	−38
150	1.29	1.69E+03	6.65E+02	0.39	−61	1.29E+03	0.77	−23
200	0.95	1.69E+03	7.55E+02	0.45	−55	1.58E+03	0.93	−7
250	0.78	1.69E+03	8.25E+02	0.49	−51	1.80E+03	1.07	7
300	0.63	1.69E+03	9.08E+02	0.54	−46	2.08E+03	1.23	23
350	0.56	1.69E+03	9.61E+02	0.57	−43	2.25E+03	1.33	33
400	0.44	1.69E+03	1.08E+03	0.64	−36	2.66E+03	1.57	57

[a] Classified by a differential mobility analyzer (DMA).

[b] Obtained from mass measurement of the DMA-classified particles by an aerosol particle mass analyzer (APM).

[c] SR means a ratio of estimated surface area to reference surface area.

TABLE 6

Estimation of surface area from total number and mass concentrations using measured effective particle densities for nearly spherical particles, assuming GSD = 1.8

Diameter[a] (nm)	Density[b] (g cm^{-3})	Reference surface area S_{cal} (cm^2 m^{-3})	DustTrak, GSD = 1.8 estimated surface area S_{est} (cm^2 m^{-3})	SR[c] (S_{est}/S_{cal})	%ΔS = 100*(S_{est} – S_{cal})/ S_{cal}	Filter, GSD = 1.8 estimated surface area S_{est} (cm^2 m^{-3})	SR (S_{est}/S_{cal})	%ΔS = 100* (S_{est} – S_{cal})/S_{cal}
50	8.61	3.30E+02	2.96E+02	0.90	−10	2.49E+02	0.76	−24
80	8.52	3.30E+02	2.97E+02	0.90	−10	2.51E+02	0.76	−24
100	8.36	3.30E+02	2.98E+02	0.90	−10	2.53E+02	0.77	−23
120	5.39	3.30E+02	3.32E+02	1.01	1	3.14E+02	0.95	−5
150	3.55	3.30E+02	3.73E+02	1.13	13	3.97E+02	1.20	20
–	1.00	3.30E+02	5.76E+02	1.75	75	8.72E+02	2.64	164

[a] Classified by a differential mobility analyzer (DMA).

[b] Obtained from mass measurement of the DMA-classified particles by an aerosol particle mass analyzer (APM) except unit density (1 g cm^{-3}).

[c] SR means a ratio of estimated surface area to reference surface area.